

17. Kostakoglu L, Elahi N, Kiratli P, et al. Clinical validation of influence p-glycoprotein on the uptake of ^{99m}Tc-sestamibi in patients with malignant tumors. *J Nucl Med* 1997;38:1003-1008.
18. Kostakoglu L, Kiratli P, Ruacan S, et al. Association of tumor wash-out rates and accumulation of ^{99m}Tc-MIBI with the expression of p-glycoprotein in lung cancer. *J Nucl Med* 1998;39:228-234.
19. Del Vecchio S, Ciarmiello A, Potena MI, et al. In vivo detection of multi-drug resistant (MDR1) phenotype by technetium-99m-sestamibi scan in untreated breast cancer patients. *Eur J Nucl Med* 1997;24:150-159.
20. Chomczynski P and Sacchi N. Single step method for RNA isolation by acid guanidiniumthiocyanate-phenol chloroform extraction. *Ann Biochem* 1979;162:156-159.
21. Nussler V, Pelka Fleischer R, Zwierzina H, et al. Clinical importance of P-glycoprotein-related resistance in leukemia and myelodysplastic syndromes first experience with their reversal. *Ann Hematol* 1994;69:S25-29.
22. Kuwazuru Y, Yoshimura A, Hanada S, et al. Expression of the multidrug transporter p-glycoprotein in acute leukemia cells and correlation to clinical drug resistance. *Cancer* 1990;66:868-873.
23. Goasguen JE, Dossot J-M, Fardel O, et al. Expression of the multidrug resistance-associated p-glycoprotein (P-170) in 59 cases of de novo acute lymphoblastic leukemia: prognostic implications. *Blood* 1993;81:2394-2398.
24. Massart C, Gibassier J, Raoul M, et al. Cyclosporin A, verapamil and S9788 reverse doxorubicin resistance in a human medullary thyroid carcinoma cell line. *Anticancer Drugs* 1995;6:135-146.
25. Stewart AJ, Canitrot Y, Baracchini E, Dean NM, Deeley RG, Cole SP. Reduction of expression of the multidrug resistance protein (MRP) in human tumor cells by antisense phosphorothioate oligonucleotides. *Biochem Pharmacol* 1996;51:461-469.
26. Webb M, Raphael CL, Asbahr H, Erber WN, Meyer BF. The detection of rhodamine 123 efflux at low levels of drug resistance. *Br J Haematol* 1996;93:650-655.
27. Delville JP, Pradier O, Pauwels O, et al. Comparative study of multidrug resistance evaluated by means of the quantitative immunohistochemical detection of P-glycoprotein and the functional release of rhodamine 123. *Am J Hematol* 1995;49:183-193.
28. Bailly JD, Muller C, Jaffrezou JP, et al. Lack of correlation between expression and function of p-glycoprotein in acute myeloid leukemia cell lines. *Leukemia* 1995;9:799-807.
29. Jain RK. Transport of molecules in the tumor interstitium: a review. *Cancer Res* 1987;47:3039-3051.
30. Hanson CA. Immunophenotyping of hematologic malignant conditions: to flow or not to flow? *Ann J Clin Pathol* 1991;96:295-298.
31. Beck WT, Grogan TM, Willman CL, et al. Methods to detect p-glycoprotein-associated multidrug resistance in patients' tumors: consensus recommendations. *Cancer Res* 1996;56:3010-3020.
32. Meleforts O, Hentze MW. Translational regulation by mRNA/protein interactions in eucaryotic cells: ferritin and beyond. *Bioassays* 1993;15:85-90.
33. Rhoads RE. Regulation of eucaryotic protein synthesis by initiation factors. *J Biol Chem* 1993;268:3017-3020.

Fluorine-18-Fluorouracil to Predict Therapy Response in Liver Metastases from Colorectal Carcinoma

Antonia Dimitrakopoulou-Strauss, Ludwig G. Strauss, Peter Schlag, Peter Hohenberger, Markus Möhler, Franz Oberdorfer and Gerhard van Kaick

Department of Oncological Diagnostics and Therapy and Department of Radiochemistry and Radiopharmacology, German Cancer Research Center, Heidelberg; Department of Internal Medicine IV, University of Heidelberg, Heidelberg; and Department of Surgery and Surgical Oncology, Virchow-Klinikum, Robert-Rössle-Klinik, Berlin, Germany

Prediction of chemotherapy response is still a problem in oncological patients. **Methods:** Studies with PET and ¹⁸F-fluorouracil (FU) were used for measurements of drug concentrations in patients with liver metastases from colorectal carcinoma. The PET data obtained before onset of FU chemotherapy were correlated to the growth rate of the metastases after therapy. The final evaluation included 25 metastases obtained in 17 patients. CT preceded the first chemotherapeutic cycle and was repeated within 3-11 mo after onset of treatment. The uptake of the cytostatic agent was evaluated in the liver metastases using the SUV at 120 min after tracer infusion. Tumor growth rate of the metastases was calculated based on CT volumetric data. **Results:** The trapping of ¹⁸F-FU was highly variable even for multiple metastases in the same patients. Six metastases with high ¹⁸F-FU uptake values exceeding 3.0 SUV correlated with negative growth rate values, 5 of 25 metastases with intermediate uptake values ranging from 2.0-3.0 SUV were associated with almost stable growth rate values nearly zero and 14 of 25 metastases with low uptake values < 2.0 SUV demonstrated positive growth rate values. Only metastases with a ¹⁸F-FU uptake exceeding 3.0 SUV at 120 min postinjection demonstrated a response to therapy. A significant correlation of 0.86 ($p < 0.001$) was found between the ¹⁸F-FU uptake values in the metastases measured before chemotherapy and the growth rate of the lesions after treatment. **Conclusion:** The data show, that FU chemotherapy outcome can be predicted using a single PET study with ¹⁸F-FU before onset to therapy.

Key Words: PET; fluorine-18-fluorouracil; liver metastases; liver treatment

J Nucl Med 1998; 39:1197-1202

Metastatic disease to the liver remains a notable problem in the treatment of oncological patients. The median survival for patients with liver metastases from colorectal cancer is 4-12 mo from the time of diagnosis of metastatic disease. The response rate to chemotherapy is highly variable (1). The standard chemotherapeutic agent used in these patients is fluorouracil (FU), which is applied as a continuous infusion or concomitant with modulators. Another approach often used in patients with inoperable liver metastases is regional chemotherapy using a surgically implanted catheter in the gastroduodenal artery (2). However, the studies published in the literature are not conclusive with respect to the therapeutic outcome (3,4). This may depend on the patient populations examined by each author, since some investigators include only patients with liver-limited disease and other with extrahepatic disease. Another point is the different doses and schemes of the chemotherapeutic protocols and especially the different technique used for intra-arterial chemotherapy.

Furthermore, the comparison of the median survival time is variably documented among authors, varying from onset of diagnosis, onset of symptoms or initiation of treatment. Some authors use different criteria to evaluate response of liver metastases to therapy, including biochemical determinants such as liver enzymes or tumor-associated antigens such as carcino-

Received Jul. 8, 1997; revision accepted Oct. 13, 1997.
For correspondence or reprints contact: Antonia Dimitrakopoulou-Strauss, MD, Department of Oncological Diagnostics and Therapy, German Cancer Research Center, Im Neuenheimer Feld 280, D-69120 Heidelberg, Germany.

embryonic antigen plasma level. The most reliable response criterion still remains the tumor volume as described by Lokich in a review on this topic (5). According to this classification a complete response is defined as a complete disappearance of all clinically recognizable tumor for a minimum of 30 days. Partial response is defined as a 50% reduction in the diameter of any lesions without demonstration of new lesions for a minimum of 30 days. A 25%–50% reduction of the tumor diameter for at least 30 days is defined as a minor response. Improvement or progression of the tumor diameter < 25% for at least 3 mo is defined as stable disease and an increase > 25% or the appearance of new lesions as progressive disease.

PET is used increasingly for obtaining quantitative data about the metabolism of malignant lesions. Metabolic studies with PET and ^{18}F -fluorodeoxyglucose (FDG) have been used not only for diagnosing liver metastases but in a limited number of patients for assessing chemotherapeutic effect. Findlay et al. (6) examined 20 patients with liver metastases from colorectal carcinoma before therapy and twice up to 5 wk after treatment with intravenous FU or modified FU therapy using alpha-interferon. Only metastases demonstrating a reduction in tumor metabolism after therapy showed a response. The authors noted a clear correlation between the reduction of the tumor metabolism 4–5 wk after initiation of treatment and the therapeutic effect. The change in the FDG uptake 1–2 wk after therapy was false-positive for response in 20% of the patients and therefore was not reliable for predicting response for therapy. One limitation of FDG PET follow-up studies for assessing therapy response is the choice of an appropriate time interval and the necessity of performing multiple follow-up studies. Another limitation of FDG PET is the delineation of treated liver metastases with a diameter smaller than 3 cm against the liver parenchyma that affects the quantification of the tumor metabolism. Treated metastases show a hypometabolic area in the center of the lesion as a result of a necrosis and a rimlike uptake in the tumor periphery, which cannot be distinguished clearly from the normal liver parenchyma.

The highly variable response rates reported in the literature, as well as the difficulties in interpretation of FDG follow-up studies, indicate the necessity for a tracer that allows a reliable distinction between responders and nonresponders at an early time after onset of therapy. Fluorine-18-FU is identical to FU and can be used for quantitative pharmacokinetic measurements in the tumor tissue and liver. In previous studies we reported on the pharmacokinetics of FU in patients with liver metastases from colorectal carcinoma using PET with ^{18}F -FU. Quantitative data on the time-activity pattern of the labeled cytostatic agent in different tissues were presented after systemic and regional application of the labeled drug (7,8). This study presents the data of ^{18}F -FU uptake measured in liver metastases before onset of therapy and tumor growth rate after initiation of FU chemotherapy. Our primary goal was to evaluate the use of only one PET study with ^{18}F -FU and a late measurement 120 min postinjection as a prognostic parameter for response to 5-FU chemotherapy.

MATERIALS AND METHODS

The final analysis comprised 17 patients and 25 metastases. The patients were examined after intravenous or intra-arterial tracer application, depending on the therapeutic protocol used for treatment. Sixteen patients included in this study suffered from nonresectable colorectal liver metastases, while 1 patient had refused resectional treatment. None of the patients had extrahepatic metastatic disease. In addition, none had undergone radiotherapy of the liver metastases. Liver metastases were confirmed by biopsy.

Nonresectability and evidence for extrahepatic disease were checked in each patient. Six of 17 patients were intended for regional chemotherapy and had surgically implanted catheters (Infuse-a-Port, Infusaid Co., Norwood, MA) in the gastroduodenal artery and a subcutaneous port system. One of these patients was included in a previous study (9). Eleven patients were scheduled for intravenous FU chemotherapy.

The standard chemotherapeutic protocol included the infusion of FU (500 mg/m²/24 hr for systemic or 1500 mg/m²/24 hr for regional therapy) for 5 days followed by a 3-wk interval without treatment. None of the patients previously had received chemotherapy. The patients were examined with PET preceding the FU therapy. Informed consent was obtained from all patients.

CT was used in all patients immediately before PET to identify the target area due to the limited field of view of the PET scanner. We used contiguous 8-mm-thick cross sections and oral contrast enhancement if required. Skin markings were made for proper repositioning of the patient for the PET study. Identical positioning supports were used for both CT and PET. CT studies preceded the first chemotherapeutic cycle and were repeated within 3–11 mo after treatment. In selected cases, contrast material was applied for diagnostic purposes. We used the nonenhanced CT studies for the calculation of tumor volume. The volume of each metastasis examined with PET was calculated from the CT slices using a three-axis method and the formula:

$\text{Vol} = (4/3) \pi \cdot a \cdot b \cdot c$, where a, b and c are the radii of the metastasis in each of three dimensions in centimeters. The growth rate was obtained from the volumetric data using the following formula:

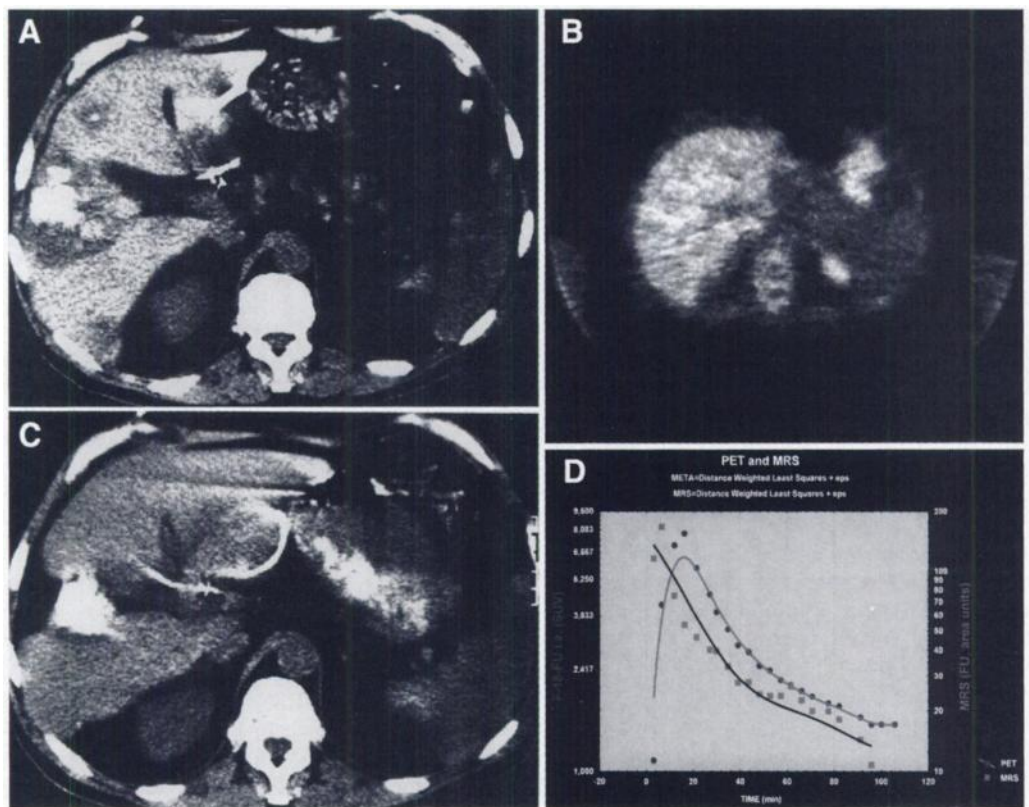
$\text{Growth rate} = \text{Ln}(\text{Vol}_2/\text{Vol}_1)/(\text{date of second CT study} - \text{date of first CT study})$,

where Vol_1 = the volume of the metastasis before chemotherapy in milliliters; Vol_2 = the volume of the metastasis after chemotherapy in milliliters; Ln = logarithmus naturalis. The unit for the growth rate is days⁻¹. Multiple CT examinations (every 3 mo) were performed in those patients included in the long-term follow-up.

A positron emission tomograph scanner with two ring detectors was used for the PET examinations. The system provides for the acquisition of three slices simultaneously, two primary sections and one cross section. Each of the two rings, of 107 cm diameter, contains 512 bismuth germanate-gadolinium orthosilicate detectors (crystal size 6 mm × 20 mm × 30 mm) and provides a 52-mm field of view. The mean sensitivity for the two primary sections is 12500 cps per $\mu\text{Ci}/\text{cm}$ (3) and 17500 cps per $\mu\text{Ci}/\text{cm}$ (3) for the secondary slice. The dead-time loss is 10% at 30000 cps per slice. The evaluation of spatial linearity showed that the maximum displacement from the ideal source position was < 0.4 mm in the whole field of view. Transmission scans with more than 10 million counts per section were obtained with a rotating germanium pin source before the first radionuclide application to obtain cross sections for the attenuation correction of the acquired emission tomographic images.

The distribution and kinetics of ^{18}F -FU were investigated with ^{18}F -FU. Fluorine-18-FU was prepared by direct fluorination of uracil in acetic acid using ^{18}F -F₂ diluted in neon (10). Quality control included high-performance liquid chromatography. Typically, 17.5 mg ^{18}F -FU was obtained with a purity > 99% and a specific activity of 1.14×10^{-5} Ci/ μM . Fluorine-18-FU (370–444 MBq) was given together with the therapeutic dose of unlabeled FU in a short, 12-min infusion either intravenously or intrarterially through the implanted port system using an infusion pump. Immediately after the ^{18}F -FU infusion was completed we infused physiologic saline through the port system. Twelve 2-min images followed by seven 5-min images and six 10-min images beginning with the FU infusion were acquired for a total acquisition time of

FIGURE 1. (A) CT cross section before onset of FU chemotherapy in patient with large calcified liver metastasis from colorectal carcinoma in lateral part of right liver lobe. (B) PET cross section 120 min after intra-arterial application of ^{18}F -FU. PET scan demonstrates nearly homogenous distribution of tracer in metastasis, which cannot be delineated from normal liver parenchyma. Intra-arterial application resulted in significantly high ^{18}F -FU trapping (5.03 SUV). (C) CT cross section in same patient 3 mo after initiation of intra-arterial chemotherapy. Significant reduction in tumor volume is demonstrated, which is in accordance with enhanced ^{18}F -FU trapping. (D) PET ^{18}F -FU interpolated time-activity data after intra-arterial tracer application and ^{19}F MRS time-signal intensity data. Downslope of both curves is parallel, which means that ^{18}F -FU uptake reflects primarily trapped nonmetabolized FU.



120 min. Appropriate skin markings were used to align the system accurately with positioning laser lights.

PET cross sections were reconstructed using an iterative reconstruction program with an image matrix of 256×256 due to the superior image quality (11). A 2-mm pixel size was chosen and a full width of half maximum of 5.1 mm was obtained in the cross sections of the patients. All images were scatter and attenuation corrected (12,13). The PET cross sections were compared to the corresponding CT slices as well as the transmission images to permit confident identification of the lesions by means of anatomic landmarks. Regions of interest (ROIs) were placed over the metastases, the normal liver parenchyma and the aorta. Only those metastases visible in 2 contiguous nonenhanced CT slices and identified in at least 2 consecutive PET slices were included in the final evaluation to minimize partial volume effects. The slice showing the largest metastasis diameter was used for the placement of the ROI. Because small lesions (< 1.5 cm) were excluded from the evaluation and respiration movement accounts for additional artifacts, no attempts were made to correct for partial volume effect. The recovery coefficient was 88% for lesions with 1.5 cm diameter.

In general, a detailed quantitative evaluation of tracer kinetics requires the use of a compartment model. However, there are no accurate models that can be used to assess ^{18}F -FU in liver metastases. The biggest problem in patient studies is obtaining the correct measurement of the input function, which demands arterial blood sampling. Another problem is the double supply of the liver through the hepatic artery and the portal vein. Therefore, we limited the evaluation to a semiquantitative approach based on the calculation of the standardized uptake value (SUV) (14): $\text{SUV} = \text{tissue concentration (MBq/g)} / [\text{injected dose (MBq)} / \text{body weight (g)}]$.

The uptake 120 min after onset of the ^{18}F -FU infusion was used for the evaluation of the trapped, nonmetabolized intracellular amount of FU, which has not been eliminated out of the tumor cells.

One of the patients planned for intra-arterial chemotherapy was examined with ^{19}F magnetic resonance spectroscopy (MRS) using the same dose and the same application route as for ^{18}F -FU PET. Fluorine-19 MRS was performed on a 1.5 Tesla whole-body MR system (Magnetom; Siemens, Erlangen, Germany). A one-turn 15-cm-diameter surface coil was placed over the liver metastasis. The field of view of the coil can be described as a 15-cm-diameter hemisphere, including a significant portion of the liver, the metastasis, muscle and subcutaneous adipose tissue. Fluorine-19 MRS spectra were recorded during and up to 90 min after the intra-arterial infusion of FU. The measurement time for each spectrum was 4.3 min. The repetition time was 1 sec, and the radiofrequency pulse length was set at 250 or 500 μsec . The ^{19}F spectrum identified two peaks by their chemical shifts: 5-FU at -93.5 parts per million (ppm) and fluoro-beta-alanine (FBAL) at -112.5 ppm. More details about the spectroscopic data are given elsewhere (15). For the comparison of the PET and MRS data in the metastasis we used only the ^{19}F -FU signal. FBAL is the major catabolite of FU formed in the normal liver parenchyma, but not in the metastasis.

Statistical evaluation of the data was performed using the Statistica software package (Version 6.0, StatSoft GmbH, Hamburg, Germany) on a Pentium 166 MHz running with Windows NT (Version 4.0, Microsoft Co., Redmond, WA).

RESULTS

Most of the liver metastases did not exhibit a significant ^{18}F -FU accumulation in the PET images and were poorly delineated as defects against the normal liver parenchyma. Visual inspection of the ^{18}F -FU images revealed a significant trapping of FU after the intra-arterial administration in only two patients. We noted large differences in the ^{18}F -FU distribution pattern for different metastases even in the same patient.

Figure 1 demonstrates an example of a liver metastasis showing a significant enhancement in the ^{18}F uptake after regional administration. We measured a high ^{18}F -FU trapping (120 min postinjection) after the onset of the ^{18}F -FU intra-

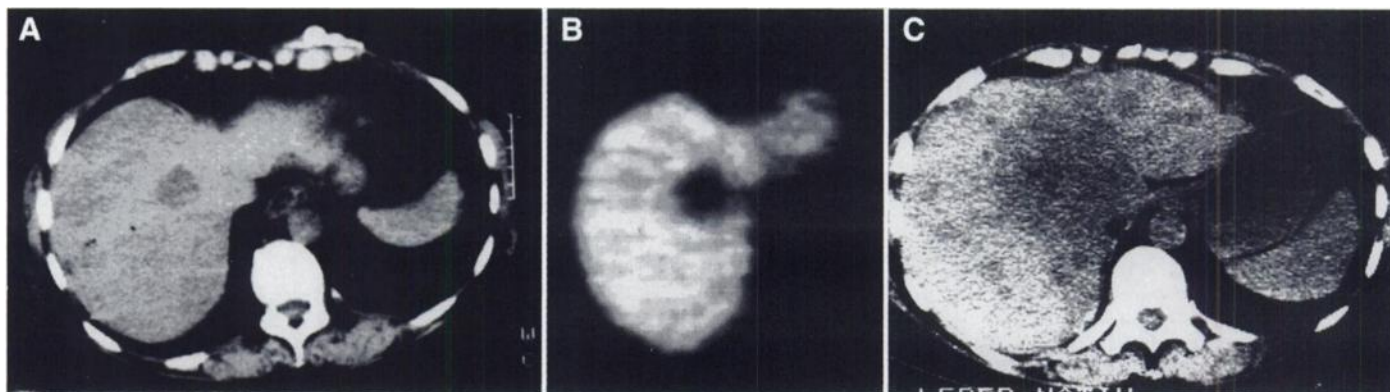


FIGURE 2. (A) CT cross section of patient with small liver metastasis in central part of cranial third of right liver lobe. Scan was performed before initiation of chemotherapy. (B) PET cross section 120 min after systemic application of ^{18}F -FU. PET scan demonstrates low trapping of ^{18}F -FU 120 min postinjection (1.91 SUV). Metastasis is delineated as defect against normal liver parenchyma. (C) CT follow-up 11 mo after initiation of FU chemotherapy. There is tremendous increase in tumor volume, which is in accordance with low ^{18}F -FU trapping values noted before therapy.

arterial infusion (Fig. 1B). The CT scans before and 3 mo after initiation of intra-arterial FU chemotherapy revealed a reduction in tumor volume (Fig. 1A, 1C). We were able to examine this patient using ^{19}F MRS. The dynamic data acquisition for ^{19}F MRS was comparable to PET. Figure 1D demonstrates the comparison of the ^{18}F time-activity curve in the metastasis and the ^{19}F time-signal curve measured in the target area. The downslope of both curves is parallel. This means, that the ^{18}F concentration measured with PET in the liver metastasis reflects primarily nonmetabolized, trapped FU. This patient responded to FU chemotherapy.

Figure 2 demonstrates an example of a liver metastasis with a low trapping of ^{18}F -FU after the systemic application (Fig. 2B). A comparison of the CT scans before onset of treatment and 3 mo after chemotherapy revealed an increase of the tumor volume and therefore a progression of disease (Fig. 2A, 2C).

The final evaluation comprises 25 metastases in 17 patients (Fig. 3). Fluorine-18-FU uptake (120 min) in the metastases varied from 1.10–5.03 SUV after the tracer administration. The highest ^{18}F -FU trapping was noted after the intra-arterial infusion of the radiolabeled drug. A comparison between the ^{18}F -FU trapping measured in the metastases before initiation of FU chemotherapy and the tumor growth rate resulted in a significant nonlinear correlation of $r = 0.86$ ($p < 0.001$) using

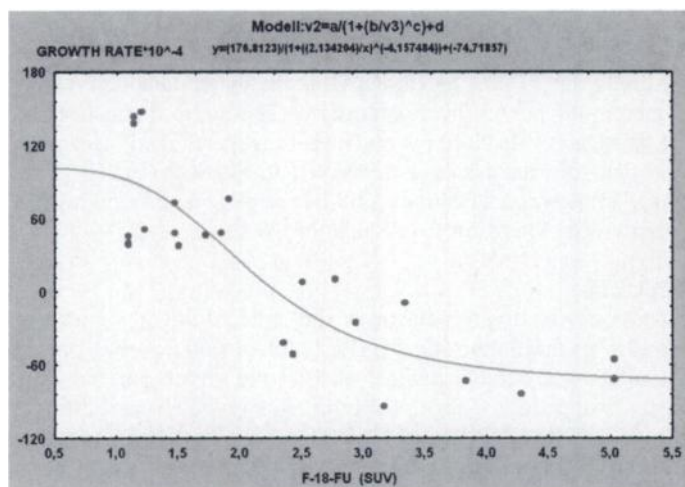


FIGURE 3. Comparison of ^{18}F -FU trapping values in SUV as measured with single PET measurement 120 min postinjection in 25 metastases from 17 patients and tumor growth rate in days^{-1} calculated with CT follow-up volumetric data. Significant correlation of 0.86 ($p < 0.001$) was found between parameters.

the equation presented in Figure 3. With respect to clinical classifications, three groups may be identified in Figure 3. Progressive disease, as demonstrated by positive growth rates is observed in all lesions < 2.0 SUV. Stable disease, as demonstrated in lesions with growth rate values nearly zero, is associated with uptake values between 2.0 and 3.0 SUV. Response to therapy as demonstrated in lesions with negative growth rate values is associated with an uptake exceeding 3.0 SUV.

DISCUSSION

This study was designed to investigate the use of a single PET study with ^{18}F -FU before treatment for the estimation of therapy outcome in patients with liver metastases from colorectal cancer. We chose a lesion-to-lesion analysis to obtain the most accurate reference for the PET data. It is known from the literature and from our previous work with labeled FU that metastases even in the same patient can show a high variation in response to chemotherapy. This is in accordance with the highly variable data reported in the literature about the response to FU chemotherapy. In the majority of studies, the change in tumor volume, the serum level of tumor markers and the survival time after onset of therapy are used as response criteria. The major limitation of this approach is the presumption that multiple metastases in the same patient will respond uniformly. This is not necessarily the case, as demonstrated in other studies (7,16). Therefore, we like to emphasize the superiority of individual growth rates for the evaluation of therapeutic effect.

Metabolic studies with PET with FDG have been used in a limited number of patients to assess therapy outcome. FDG follow-up studies were performed in patients with treated malignant lymphomas to evaluate chemotherapy outcome before blood stem cell support (17). The use of at least three follow-up PET FDG studies and a dedicated data analysis were mandatory to identify responders earlier than morphological imaging modalities. The authors emphasized the need of at least three follow-up studies for prediction of therapy outcome, which is a limitation of the PET FDG technique. Findlay et al. (6) used FDG studies to evaluate the outcome of FU chemotherapy in 20 patients with liver metastases from colorectal cancer. The authors examined all patients before, 1–2 wk and 4–5 wk after initiation of FU chemotherapy. They noted a correlation between the 4–5-wk tumor-to-liver (T/L) ratio and therapy outcome using both a lesion-to-lesion analysis as well as an overall patient response assessment with a sensitivity of 100% and a specificity of 90% and 75%, respectively. Interest-

ingly, neither the pretreatment T/L ratio nor the 1–2-wk ratio correlated to therapy outcome. Furthermore, the authors observed an overall increase of the FDG metabolism in 3 lesions of the responding group and a marked reduction in 2 lesions in the nonresponding group. The study confirms some limitations of the FDG follow-up studies, like the so called “flare phenomenon” shortly after initiation of chemotherapy and the importance of the correct choice of a time interval for the PET study after therapy to evaluate therapy response.

FU is still the most important cytostatic agent for the therapy of metastatic colorectal cancer. Different modified protocols are in use, which include pretreatment with modulators such as folinic acid or regional drug administration through surgically implanted catheters (1,2,18,19). The response to these treatment modalities was highly variable and the mean survival time was equivalent to the classic systemic application (1,2,4). This indicates the need of a method that can help to choose the most effective treatment protocol in each patient and carefully assess the expected benefit. Modified treatment protocols, such as pretreatment with folinic acid, are only suitable when a drug has already shown a significant cytostatic effect in the systemic setting of application. Therefore, the goal of modified protocols would be to push some partial responses to complete response and some minimal response into at least partial response. For this purpose it is helpful to assess individual drug concentrations at the target area before onset of therapy (7).

PET with ^{18}F -FU enables direct measurements of the distribution of the cytostatic agent, since ^{18}F -FU is biochemically identical with the nonlabeled drug. In previous studies we reported the pharmacokinetics of FU after systemic and/or regional administration in patients with liver metastases from colorectal cancer, using the same dose of nonlabeled FU (7,9). After the systemic application of ^{18}F -FU 14.1% (11/78) of liver metastases demonstrated an FU trapping exceeding 2.0 SUV. The mean SUV in the liver metastases 120 min postinjection was 1.39 SUV (50 patients, 78 metastases) and approximately one-third of the mean SUV in the normal liver parenchyma. We reported that the highest ^{18}F -FU concentrations were measured after the intra-arterial administration with a maximal uptake of 5.03 SUV for the ^{18}F -FU trapping 120 min postinjection. The comparison of the systemic and the intra-arterial administration of the same dose of FU in 15 patients and 24 metastases demonstrated an enhanced trapping in one-third (8/24) of all metastases, despite the fact that the access was improved by a factor of five after intra-arterial administration. The data showed that the cytostatic agent is eliminated quickly from the tumor cells, despite the better access and the enhanced local concentration of the drug in the early phase. The major limiting parameter for an enhanced trapping is the high elimination of FU out of the tumor cells, which was not saturable with the usual FU dose used in patients. Furthermore, an intravenous PET study with ^{18}F -FU was not predictive for the pharmacokinetics of the drug after the intra-arterial administration or pretreatment.

The aim of this study was to investigate whether one PET study with ^{18}F -FU is predictive for therapy outcome. We examined all patients included in the study using the same dose and the same application route as for therapy. Patients planned for intra-arterial FU chemotherapy were studied after the intra-arterial infusion of ^{18}F -FU through the surgically implanted catheter. Patients scheduled for intravenous FU treatment were studied using the systemic application of the drug. Labeled FU was mixed with the therapeutic dose of cold FU to simulate the chemotherapy situation. One critical point is the selection of the appropriate time intervals for the evaluation of

clinically relevant pharmacokinetic parameters for the FU data, like the trapping of the cytostatic agent. We showed in a previous work that late FU uptake values (120 min) represent the amount of trapped nonmetabolized FU when the systemic administration was selected (7,9,16). Chaudhuri et al. (20) examined the FU pathway in mice bearing sarcoma-180 and reported that even 60 min after injection of 25 mg/kg FU, 61% of the radioactivity in the tumor represents nonmetabolized FU. Late images obtained 120 min after the systemic ^{18}F -FU administration are most likely to represent trapped nonmetabolized FU. It should be noted that therapeutically inactive FU catabolites, like alpha-fluoro-beta-alanine, have only been detected in the normal liver parenchyma but not in the metastases (15). According to these considerations, we chose a late measurement 120 min after tracer application and correlated the ^{18}F -FU uptake at this time to the growth rate of the lesions after initiation of chemotherapy.

Several authors tried to correlate the FU uptake with the response to therapy using animal studies. Wolf et al. (21) studied the kinetics of FU in some patients as well as in rabbits bearing VX2 tumors using F-19 MRS up to 120 min postinjection. He noted a significant trapping of nonmetabolized FU in some human tumors. The amount of trapped FU correlated with therapy outcome. This is in accordance with the spectroscopic data of the patient presented in Figure 1D. Fluorine-19 MRS allows general differentiation between 5-FU and its metabolites. The major limitation of MRS is its intrinsically low sensitivity. Furthermore, the applied surface coil technique, as used for this study, does not allow secure discrimination between signals originating from the liver and those from tumor tissue. In the presented MRS study, we clearly recognized two spectra: one for the FU and a second one for FBAL. Fluorine-19 MRS demonstrated initially a high FU-signal, followed by an increase of the main catabolite, FBAL. We assumed that the FBAL signal originates from the normal surrounding liver tissue, as known from experimental studies and used the data of the ^{19}F -FU signal for comparison to PET. The downslope of the ^{18}F time-activity curve for the metastases was comparable to the time-signal curve for FU obtained by MRS. This may indicate, that the ^{18}F -FU accumulation in the metastases reflects primarily nonmetabolized, trapped FU.

Shani and Wolf (22) examined the FU uptake in two variants of the same tumor in mice: In the solid L-1210 lymphocytic leukemia tumor, susceptible to FU and in a tumor line resistant to FU. The authors noted mean tumor-to-blood ratios of 1.9 2 hr after intravenous FU injection in the sensitive line and 0.96 in the resistant tumor. The difference was even greater 12 hr postinjection with a ratio of 20.69 for the sensitive and 4.04 for the resistant tumors, respectively. The data support the hypothesis that tumor response is associated with high FU uptake in the late phase, at least 1 hr after the FU application. The data are in accordance to the results of this study. Fluorine-18-FU uptake measured with PET before therapy correlated with the tumor growth rate as calculated using volumetric data from CT follow-up studies after initiation of therapy. Lesions showing a positive growth rate and, therefore, no response to the FU treatment demonstrated uptake values below 2.0 SUV before therapy. In contrast, lesions with a negative growth rate, which responded to FU chemotherapy showed uptake values exceeding 3.0 SUV. Intermediate uptake values correlated to growth rate values nearby zero.

PET studies with ^{18}F -FU are a useful tool for therapy management in patients with metastatic colorectal cancer and can help to optimize and individualize the chemotherapeutic treatment. The use of ^{18}F -FU is superior to FDG, because only

one ^{18}F -FU study 120 min postinjection is required, and the radiotracer reflects the distribution of the cytostatic agent and the trapping which is predictive to therapy outcome.

CONCLUSION

Studies with ^{18}F -FU in patients with metastatic colorectal carcinomas have shown, that PET is a suitable tool for pharmacokinetic studies, since ^{18}F -labeled FU is identical to the nonlabeled agent. In this study, we compared the trapping of ^{18}F -FU in liver metastases before onset of chemotherapy with the tumor growth rate as measured by CT follow-up studies within 3–11 mo after initiation of FU chemotherapy. Only lesions with an enhanced trapping of ^{18}F -FU (120 min postinjection) exceeding 3.0 SUV responded to therapy. A significant correlation of 0.86 ($p < 0.001$) was found between the ^{18}F -FU trapping and the tumor growth rate. PET with ^{18}F -FU and a single measurement 120 min postinjection before onset of chemotherapy helps to identify responders and nonresponders and, therefore, predict therapy effect.

ACKNOWLEDGMENTS

We thank Professor Wolfhard Semmler, MD, PhD, at the Institute of Diagnostics and Research, Berlin and Peter Bachert, PhD, of the MR group, Department of Biophysics and Medical Radiation Physics, German Cancer Research Center, Heidelberg for performing the MR spectroscopic study.

REFERENCES

1. Kemeny N. The systemic chemotherapy of hepatic metastases. *Semin Oncol* 1983;10:148–158.
2. Niederhuber JE, Ensminger WD. Surgical consideration in the management of hepatic neoplasia. *Semin Oncol* 1983;10:135–147.
3. Huberman MS. Comparison of systemic chemotherapy with hepatic arterial infusion in metastatic colorectal carcinoma. *Semin Oncol* 1983;10:238–248.
4. Vaughn DJ, Haller DG. Nonsurgical management of recurrent colorectal cancer. *Cancer* 1993;71:4278–4292.
5. Lokich JL. Determination of response in treatment of hepatic neoplasia. *Semin Oncol* 1983;10:228–237.
6. Findlay M, Young H, Cunningham D, et al. Noninvasive monitoring of tumor metabolism using fluorodeoxyglucose and positron emission tomography in colorectal cancer liver metastases: correlation with tumor response to fluorouracil. *J Clin Oncol* 1996;14:700–708.
7. Dimitrakopoulou A, Strauss LG, Clorius JH, et al. Studies with positron emission tomography after systemic administration of fluorine-18-uracil in patients with liver metastases from colorectal carcinoma. *J Nucl Med* 1993;34:1075–1081.
8. Strauss LG, Conti PS. The applications of PET in clinical oncology. *J Nucl Med* 1991;32:623–648.
9. Dimitrakopoulou-Strauss A, Strauss LG, Schlag P, et al. Intravenous and Intrarterial O-15-H₂O and ^{18}F -fluorouracil in patients with metastatic colorectal cancer. *J Nucl Med* 1998;39:465–473.
10. Oberdorfer F, Hofmann E, Maier-Borst W. Preparation of ^{18}F -labeled 5-fluorouracil of very high purity. *J Lab Compds Radiopharm* 1989;27:137–145.
11. Doll J, Ostertag HJ, Bellemann ME, et al. Effects of distorted PET projection data on the reconstructed image using different reconstruction algorithms. In: Bergmann H, Sinzinger H eds. *Radioactive isotopes in clinical medicine and research advances in pharmacological sciences*. Basel: Birkhäuser Verlag; 1995:85–90.
12. Ostertag H, Kübler WK, Doll J, Lorenz WJ. Measured attenuation correction methods. *Eur J Nucl Med* 1989;15:722–726.
13. Hoverath H, Kübler WK, Ostertag H, et al. Scatter correction in the transaxial slices of a whole-body positron emission tomograph. *Phys Med Biol* 1993;717–728.
14. Strauss LG, Clorius JH, Schlag P, et al. Recurrence of colorectal tumors: PET evaluation. *Radiology* 1989;170:329–332.
15. Semmler W, Bachert-Baumann P, Gückel F, et al. Real-time follow-up of 5-fluorouracil metabolism in the liver of tumor patients by means of F-19 MR spectroscopy. *Radiology* 1990;174:141–145.
16. Strauss LG. Application of positron emission tomography in colorectal carcinoma. *Onkologie* 1993;16:232–244.
17. Dimitrakopoulou-Strauss A, Strauss LG, Goldschmidt H, Lorenz WJ, Maier-Borst W, van Kaick G. Evaluation of tumour metabolism and multidrug resistance in patients with treated malignant lymphomas. *Eur J Nucl Med* 1995;22:434–442.
18. Boyle FM, Smith RC, Levi JA. Continuous hepatic artery infusion of 5-fluorouracil for metastatic colorectal cancer localised to the liver. *Aust N Z J Med* 1993;23:32–34.
19. De Takats PG, Kerr DJ, Poole CJ, et al. Hepatic arterial chemotherapy for metastatic colorectal carcinoma. *Br J Cancer* 1994;69:372–378.
20. Chaudhuri NK, Murkherjee KL, Heidelberger C. Studies of fluorinated pyrimidines-VII-the degradative pathway. *Biochem Pharmacol* 1959;1:328–341.
21. Wolf W, Presant CA, Servis KL, et al. Tumor trapping of 5-fluorouracil: In vivo ^{19}F NMR spectroscopic pharmacokinetics in tumor-bearing humans and rabbits. *Proc Natl Acad Sci USA* 1990;87:492–496.
22. Shani J, Wolf W. A model for prediction of chemotherapy response to 5-fluorouracil based on the differentiated distribution of 5- ^{18}F -fluorouracil in sensitive versus resistant lymphocytic leukemia in mice. *Cancer Res* 1977;37:2306–2308.

Severe Thyrotoxicosis Due to Functioning Pulmonary Metastases of Well-Differentiated Thyroid Cancer

Massimo Salvatori, Ida Saletnich, Vittoria Rufini, Massimo E. Dottorini, Salvatore M. Corsello, Luigi Troncone and Brahm Shapiro

Istituto di Medicina Nucleare e di Endocrinologia, Università Cattolica del Sacro Cuore, Roma; U.O. Medicina Nucleare, Ospedale di Circolo, Busto Arsizio, Roma, Italy; and Division of Nuclear Medicine, Department of Internal Medicine, University of Michigan Medical Center, Ann Arbor, Michigan

We report two cases of thyrotoxicosis resulting from hyperfunctioning lung metastases from differentiated thyroid cancer. In both patients, a simultaneous diagnosis of thyrotoxicosis and metastatic thyroid cancer was made, based on thyroid function tests as well as ^{131}I whole-body scans showing low thyroid uptake of radioiodine and multiple foci of intense ^{131}I uptake in the lungs. After total thyroidectomy (performed in Patient 2 only) and ^{131}I therapy (cumulative dose of 12.3 GBq in Patient 1 and 9.6 GBq in Patient 2), there was a rapid clinical improvement with significant reduction of the pulmonary metastatic disease in both patients: Patient 1 became euthyroid, while Patient 2 became hypothyroid. Analysis of the 54 cases reported in the literature, including the 2 cases described

here, shows this to be a very rare cause of thyrotoxicosis and one that can pose serious problems for both the diagnostic evaluation and choice of therapeutic strategy when compared with the much more common nonhyperfunctioning metastases from thyroid cancer. Lesser degrees of thyroid hormone secretion by differentiated thyroid cancer may be detected and exploited diagnostically by the chromatographic analysis of serum for endogenously labeled thyroid hormones after ^{131}I administration.

Key Words: thyrotoxicosis; differentiated thyroid cancer; lung metastases; iodine-131 therapy

J Nucl Med 1998; 39:1202–1207

Thyrotoxicosis resulting from functioning metastatic thyroid cancer is rare. In 1946, Leiter et al. (1) described the first

Received Feb. 25, 1997; revision accepted Oct. 13, 1997.
For correspondence or reprints contact: Massimo Salvatori, MD, Istituto di Medicina Nucleare, Policlinico A. Gemelli, Largo A. Gemelli 8, 00168 Roma, Italy.